

Splice variant of the SND1 transcription factor is a dominant negative of SND1 members and their regulation in *Populus trichocarpa*

Quanzi Li^{a,1}, Ying-Chung Lin^{a,1}, Ying-Hsuan Sun^a, Jian Song^a, Hao Chen^a, Xing-Hai Zhang^b, Ronald R. Sederoff^{a,2}, and Vincent L. Chiang^{a,2}

^aForest Biotechnology Group, Department of Forestry and Environmental Resources, North Carolina State University, Raleigh, NC 27695; and ^bDepartment of Biological Sciences, Florida Atlantic University, Boca Raton, FL 33431

Contributed by Ronald R. Sederoff, July 27, 2012 (sent for review July 2, 2012)

Secondary Wall-Associated NAC Domain 1s (SND1s) are transcription factors (TFs) known to activate a cascade of TF and pathway genes affecting secondary cell wall biosynthesis (xylogenesis) in *Arabidopsis* and poplars. Elevated SND1 transcriptional activation leads to ectopic xylogenesis and stunted growth. Nothing is known about the upstream regulators of *SND1*. Here we report the discovery of a stem-differentiating xylem (SDX)-specific alternative *SND1* splice variant, *PtrSND1-A2^{IR}*, that acts as a dominant negative of *SND1* transcriptional network genes in *Populus trichocarpa*. *PtrSND1-A2^{IR}* derives from *PtrSND1-A2*, one of the four fully spliced *PtrSND1* gene family members (*PtrSND1-A1*, *-A2*, *-B1*, and *-B2*). Each full-size *PtrSND1* activates its own gene, and all four full-size members activate a common *MYB* gene (*PtrMYB021*). *PtrSND1-A2^{IR}* represses the expression of its *PtrSND1* member genes and *PtrMYB021*. Repression of the autoregulation of a TF family by its only splice variant has not been previously reported in plants. *PtrSND1-A2^{IR}* lacks DNA binding and transactivation abilities but retains dimerization capability. *PtrSND1-A2^{IR}* is localized exclusively in cytoplasmic foci. In the presence of any full-size *PtrSND1* member, *PtrSND1-A2^{IR}* is translocated into the nucleus exclusively as a heterodimeric partner with full-size *PtrSND1*s. Our findings are consistent with a model in which the translocated *PtrSND1-A2^{IR}* lacking DNA-binding and transactivating abilities can disrupt the function of full-size *PtrSND1*s, making them nonproductive through heterodimerization, and thereby modulating the *SND1* transcriptional network. *PtrSND1-A2^{IR}* may contribute to transcriptional homeostasis to avoid deleterious effects on xylogenesis and plant growth.

Wood is an important source of materials and energy. Wood formation is a result of the regulated accumulation of secondary xylem cells (fibers, vessels, and rays in dicots) differentiated from the vascular cambium (1). Differentiation of these cells involves wall thickening accompanied by the biosynthesis of wall components, lignin, cellulose, and hemicelluloses, and it is terminated by programmed cell death (1). Regulation of wood formation is known at the level of transcription factors (TFs). A small group of NAC TFs is implicated in wood formation (2, 3). Much of this knowledge was derived from recent work on xylogenesis in *Arabidopsis* (4–6).

Approximately 110 NAC genes are found in the *Arabidopsis* genome. Of these, five are named SND (Secondary Wall-Associated NAC Domain) (7), and seven are named VND (Vascular-Related NAC Domain) (8, 9). SNDs play more specific roles in fiber cell differentiation, and VNDs are activators of vessel formation. SND1 and VND6/7 can each activate the expression of the same set of 12 downstream TF genes, mostly MYBs (5, 6). SND1 and VND6/7 can also directly or indirectly activate genes associated with lignin, cellulose, and hemicellulose biosynthesis through other TFs that are also part of the secondary cell wall biosynthesis regulatory network (5, 6). In this network, higher-level (such as transacting factors) regulation of SND1 and VND6/7 is expected to prevent these NACs from activating the transcription of a cascade of TFs and pathway genes. When this transcriptional homeostasis is not maintained, stunted growth, ectopic secondary

cell wall thickening, and deposition of wall components result, as demonstrated by overexpression of *SND* and *VND* genes in *Arabidopsis* or poplar (2). However, nothing is known about the higher-level regulation of SND or VND.

Most TFs, including NACs, dimerize to transactivate target genes in the nucleus (10). After protein synthesis in the cytoplasm, TF translocation as monomers or dimers into the nucleus therefore offers fundamental strategies for transcriptional regulation (10, 11). A few NACs, such as *Arabidopsis* SND1 and VND6, were shown to be in the nucleus (7, 9, 12, 13), but, surprisingly, the subcellular locations of NAC dimers have never been demonstrated. Knowledge about nucleocytoplasmic transport, including the monomer-to-dimer transition of SNDs and VNDs, is central to a more comprehensive understanding of transcriptional regulation in xylogenesis.

Transcriptional repression through repressor and corepressor TFs is also a useful mechanism for maintaining transcriptional homeostasis (14, 15). Many such TFs are dominant negatives derived from mutations or alternative splicing that disrupt TFs' DNA-binding function, but not their protein–protein interaction or dimerization ability (16, 17). The defective TF can still heterodimerize or homodimerize with a functional TF, forming a complex where there is only one DNA-binding or activation domain instead of the required two, resulting in nonfunctional protein complexes (15, 17, 18). Both dominant-negative mutations and splice variants of TFs have been extensively studied in animals (15–18). In plants, there are two very recent reports on two alternative splice forms in *Arabidopsis* TFs that act as regulators inhibiting their full-size gene product from activating a direct downstream target (19, 20). In animals, a dominant negative is often an antagonist of a set of targets or of multiple members of a TF family (17, 18). This more effective means of maintaining transcriptional homeostasis, which may be important for regulating hierarchical transcriptional networks, has yet to be demonstrated in plants.

Here we describe the discovery of naturally occurring alternative splicing of *PtrSND1-A2*, a *Populus trichocarpa* *SND1* gene family member. The splice variant *PtrSND1-A2^{IR}* is shown to be a negative regulator of multiple *PtrSND1* gene family members and a *MYB* gene—a direct target of these members. We conducted transient transcriptional perturbation in *P. trichocarpa* stem-differentiating xylem (SDX) protoplasts, transactivation, and electrophoretic mobility shift assays (EMSAs). The findings were integrated with results of SDX subcellular protein colocalization and translocation, yeast two-hybridization (Y2H), and bimolecular fluorescence

Author contributions: Q.L., Y.-C.L., R.R.S., and V.L.C. designed research; Q.L., Y.-C.L., Y.-H.S., J.S., H.C., and X.-H.Z. performed research; Q.L., Y.-C.L., Y.-H.S., R.R.S., and V.L.C. analyzed data; and Q.L., Y.-C.L., Y.-H.S., R.R.S., and V.L.C. wrote the paper.

The authors declare no conflict of interest.

¹Q.L. and Y.-C.L. contributed equally to this work.

²To whom correspondence may be addressed. E-mail: vchiang@ncsu.edu or ron_sederoff@ncsu.edu.

This article contains supporting information online at www.pnas.org/lookup/suppl/doi:10.1073/pnas.1212977109/-DCSupplemental.

complementation (BiFC) to provide further evidence for the unique regulatory function of this splice variant.

Results

Naturally Occurring Splice Variant of a *PtrSND1* Gene Was Identified Through PCR Cloning, RNA Sequencing (RNA-Seq), and 3' Rapid Amplification of cDNA Ends (RACE). We identified 20 *SND* and *VND* homologs in *P. trichocarpa* and demonstrated that essentially all of them are preferentially expressed in SDX (Fig. S1 and Table S1). We focused on all four *SND1* homologs, which we named *PtrSND1-A1* (POPTR_0011s15640; also named *PtVNS12/PtrWND1A*; refs. 2 and 3), *PtrSND1-A2* (POPTR_0001s45250; *PtVNS11/PtrWND1B*; refs. 2 and 3), *PtrSND1-B1* (POPTR_0014s10060; *PtVNS09/PtrWND2A*; refs. 2 and 3), and *PtrSND1-B2* (POPTR_0002s17950; *PtVNS10/PtrWND2B*; refs. 2 and 3). *PtrSND1-A1* and *-A2* share 90.1% protein sequence identity (Fig. S2) and are phylogenetically paired gene members, as are *PtrSND1-B1* and *-B2* (81.9% protein sequence identity). We then cloned the cDNAs of these four member genes to study their transcriptional functions.

These four genes have a typical *NAC* gene structure of three exons and two introns, encoding cDNAs of ~1.2–1.3 kb. The cDNA with the expected size for each of the four *PtrSND1*s was PCR-amplified from SDX (Fig. 1A) and verified by sequencing. There was a larger product (~1.7 kb) from *PtrSND1-A2* (Fig. 1A) that retained the second intron from incomplete splicing of the *PtrSND1-A2* gene (Version 2.0; <http://www.phytozome.org>). The 1.7-kb cDNA variant is more abundant in SDX than in phloem, young shoots, and roots (Fig. 1B). We readily PCR-amplified this 1.7-kb cDNA from the SDX of 12 independent *P. trichocarpa* plants (6–9 mo old) maintained under normal greenhouse

conditions and tested at different times. Furthermore, RNA-seq of the SDX transcripts of another set of three *P. trichocarpa* plants confirmed the inclusion of intron 2 in the *PtrSND1-A2* mRNA (Fig. 1C and D). Essentially, no intron sequence reads were found for *PtrSND1-A1*, *-B1*, or *-B2* mRNAs (Fig. S3).

We next tested whether the cloned 1.7-kb intron-retaining cDNA was derived from the mature mRNA. We conducted 3' RACE PCR on SDX RNAs to amplify sequences flanking ATG and poly(A) tail (Fig. 1E, *ii* and *iii*) and obtained three products (Fig. 1F). Sequencing of these products verified that each had a 3' poly(A) tail. The largest product (~1.9 kb; Fig. 1F) included the sequence of the second intron of the *PtrSND1-A2* gene (Fig. 1E, *iii*)—a poly(A)-tailed version of the 1.7-kb cDNA described above. The other two products (Fig. 1F) had no introns (Fig. 1E, *ii*) but encoded an identical protein, and their size difference was due to the different polyadenylation sites on the completely spliced *PtrSND1-A2* mRNA. For each of the other three *PtrSND1*s, 3' RACE PCR resulted in amplification of only the full cDNA. These results demonstrated that this alternative splicing event occurs consistently and naturally, derived from a gene-member-specific mature mRNA that shows SDX specificity. We named this Intron Retained splice variant *PtrSND1-A2^{IR}*, a unique transcript of the *PtrSND1* family.

Splice Variant *PtrSND1-A2^{IR}* Encodes a Unique NAC-Domain Protein in *P. trichocarpa* SDX cells. We next analyzed whether the *PtrSND1-A2^{IR}* mRNA is processed for protein production. The full-size *PtrSND1-A2* cDNA was predicted to produce a protein of 418 amino acids (aa) with a conserved N-terminal NAC domain (180 aa) and a C-terminal activation domain (238 aa) (refs. 12 and 22; Fig. 1E, *iv*). The NAC domain is encoded by exons 1 and 2 and the

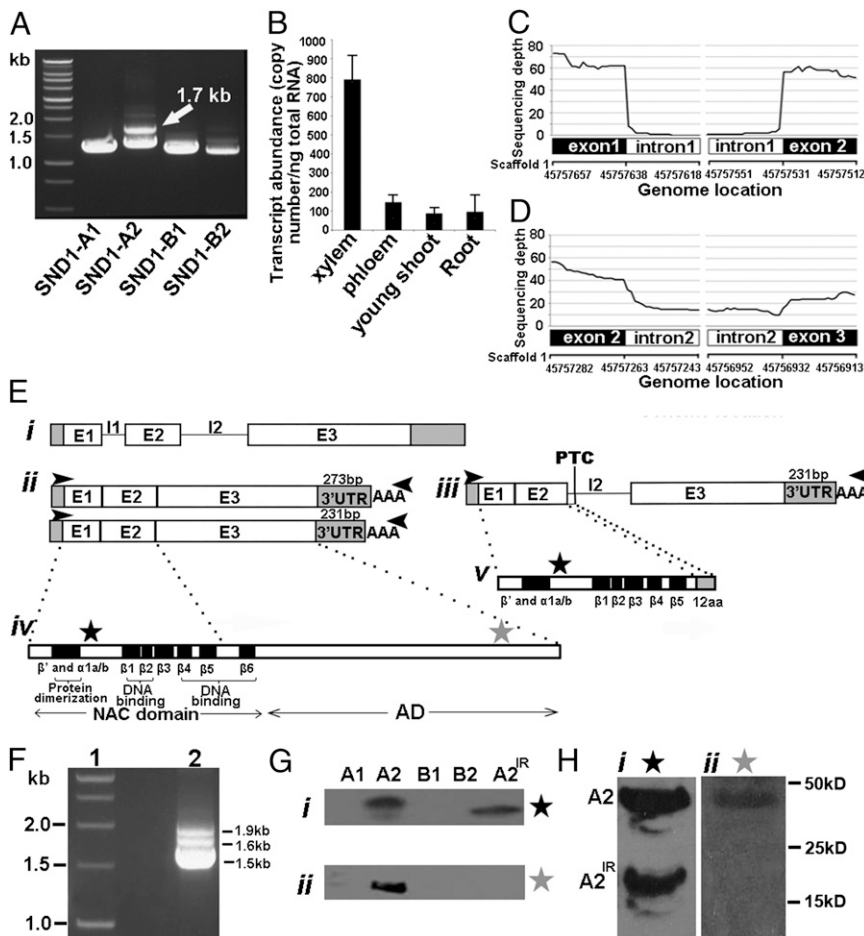


Fig. 1. Discovery of *PtrSND1-A2^{IR}*. (A) PCR of *PtrSND1* members *PtrSND1-A1* (A1), *PtrSND1-A2* (A2), *PtrSND1-B1* (B1), and *PtrSND1-B2* (B2). (B) qRT-PCR of *PtrSND1-A2^{IR}* (*A2^{IR}*) tissue-specific expression. (C and D) RNA-seq analysis of *PtrSND1-A2*. (C) The 20 nt in intron 1 immediately after exon 1 or before exon 2 has essentially zero reads, i.e., no intron. (D) The 20 nt in intron 2 has an average sequencing depth of 16 reads, and the 20 nt in exons 2 and 3 has 37 reads (~1 intron read in every 2 exon reads), confirming retention of intron 2. (E) Gene and protein structures of A2 and *A2^{IR}*. (i) A2 genomic DNA with three exons (E1–E3) and two introns (I1 and I2). (ii) Two A2 mRNAs with different length of 3'UTR. (iii) *A2^{IR}* mRNA with a retained intron 2 having a premature termination codon (PTC). (iv) A2 protein with an N-terminal NAC domain consisting of β', α1a/b, and β1–β6 subdomains and a C-terminal activation domain (AD). (v) *A2^{IR}* protein, containing β', α1a/b, β1–β5, and 12 aa, but lacking β6 and AD. (F) 3' RACE PCR of A2 and *A2^{IR}*. Lane 1, size marker; lane 2, PCR products from A2 (1.5 and 1.6 kb) and *A2^{IR}* (1.9 kb). The forward and reverse primers are shown as left and right arrowheads in E, *ii* and *iii*. (G) Western blot for antibody specificity. (i) *E. coli* produced recombinant NAC-domain proteins from A1, A2, B1, B2, and recombinant protein of the full-length *A2^{IR}*, probed with the NAC-domain antibody (black star) located in the NAC domain of A2 (E, *iv*) and *A2^{IR}* (E, *v*). (ii) Purified full-length A1, A2, B1, B2, and *A2^{IR}* recombinant proteins from *E. coli* probed with the C-terminal antibody (gray star) located at the C terminus of A2 (E, *iv*). (H) Western blot analysis of SDX total organelle proteins probed with the NAC-domain antibody (black star) (i) and probed with the C-terminal antibody (gray star) (ii).

$\beta 6$ subdomain from exon 3 (22). The activation domain is encoded by the exon 3 portion without the $\beta 6$ sequence. The *PtrSND1-A2^{IR}* cDNA (1.9 kb; Fig. 1F) encodes a predicted protein of only 166 aa because of a premature termination codon (PTC) (Fig. 1E, iii) in the retained intron 2. As a result, PtrSND1-A2^{IR} would be a NAC-domain protein that has no activation domain but has a protein dimerization domain (β' and $\alpha 1(a/b)$), $\beta 1$ – $\beta 5$ subdomains, and a unique C terminus of 12 aa translated from the retained intron 2 portion upstream of the PTC (Fig. 1E, v).

We then performed Western blot analysis to test for the presence of PtrSND1-A2^{IR} protein. Protein-specific polypeptides (Fig. 1E, iv and v) were selected as immunogens to make antibodies that would distinguish PtrSND1-A2^{IR} and -A2 and discriminate these from the other three full-size PtrSND1 proteins. Antibody specificity was validated against *Escherichia coli* recombinant proteins from the five *PtrSND1* genes (Fig. 1G, i). The SDX proteins gave two bands with sizes corresponding to the predicted molecular masses of PtrSND1-A2 (47.2 kDa) and PtrSND1-A2^{IR} (19.5 kDa), respectively, by using antibodies that would recognize the NAC domain of these two proteins (Fig. 1H, i) but not of the other three PtrSND1s (Fig. 1G, i). The identity of these two proteins was further discriminated by anti-PtrSND1-A2-specific antibody (Fig. 1H, ii). These results demonstrate the presence of a unique NAC protein, PtrSND1-A2^{IR}, in *P. trichocarpa* SDX. We then characterized the function of this protein and its regulatory relationship with the other four full-size PtrSND1 members.

PtrSND1-A2^{IR} Inhibits *PtrMYB021* Gene Expression. In *Arabidopsis*, SND1 activates directly the expression of *AtMYB46* and *AtMYB83* (23). We tested whether all five *P. trichocarpa* SND1 members (including PtrSND1-A2^{IR}) can directly transactivate *MYB* gene expression in *P. trichocarpa*. We focused on *PtrMYB021* (POPTR_0009s05860), the ortholog of *AtMYB46* (24). We overexpressed each of the five *PtrSND1* genes in *P. trichocarpa* SDX protoplasts, using protocols that we recently developed (25). All four full-size PtrSND1s could induce a twofold to fourfold increase in abundance of endogenous *PtrMYB021* transcripts in SDX protoplasts (Fig. 2A), consistent with the known *SND1*-mediated transactivation of *MYB* targets. In contrast, overexpression of *PtrSND1-A2^{IR}* significantly reduced the *PtrMYB021* transcript level (Fig. 2A). A repression of *MYB* expression by any fully spliced *SND1* has not been previously detected. Effector–reporter-based gene transactivation assays further suggested that the observed induction of *PtrMYB021* expression was a result of the activation of the *PtrMYB021* promoter by the PtrSND1 member (Fig. 2B). The assays also showed that PtrSND1-A2^{IR} could not activate the *PtrMYB021* promoter, consistent with the lack of an activation domain in PtrSND1-A2^{IR} and suggesting that the observed PtrSND1-A2^{IR}-mediated suppression of *PtrMYB021* expression (Fig. 2A) operates by other repression mechanisms.

We next used EMSA to test whether the PtrSND1-mediated transactivation of *PtrMYB021* is a result of direct binding of PtrSND1 to the *PtrMYB021* promoter. Retardation of DNA probe mobility and probe competition demonstrated that each of the four full-size PtrSND1 members can directly bind to a conserved sequence motif in the *PtrMYB021* promoter (Fig. 2C and Fig. S4). However, PtrSND1-A2^{IR} did not bind to the *PtrMYB021* promoter (Fig. 2C). The lack of DNA-binding ability suggests that the $\beta 6$ subdomain (22, 26), which is missing in PtrSND1-A2^{IR} (Fig. 1E, v), plays an important role in DNA binding. These results confirm that *PtrMYB021* is a common and direct transactivation target of the four full-size PtrSND1 members. Transactivation and EMSA results revealed that the splice variant PtrSND1-A2^{IR} negatively regulates *PtrMYB021* gene expression through a mechanism that is independent of an activation domain and direct *PtrMYB021* DNA-binding ability in PtrSND1-A2^{IR}.

PtrSND1-A2^{IR} Inhibits the Expression of *PtrSND1* Gene Members. We investigated further the regulatory role of PtrSND1-A2^{IR} by testing whether PtrSND1-A2^{IR} can also affect the expression of the other four *PtrSND1* members. Overexpression of *PtrSND1-A2^{IR}* in *P.*

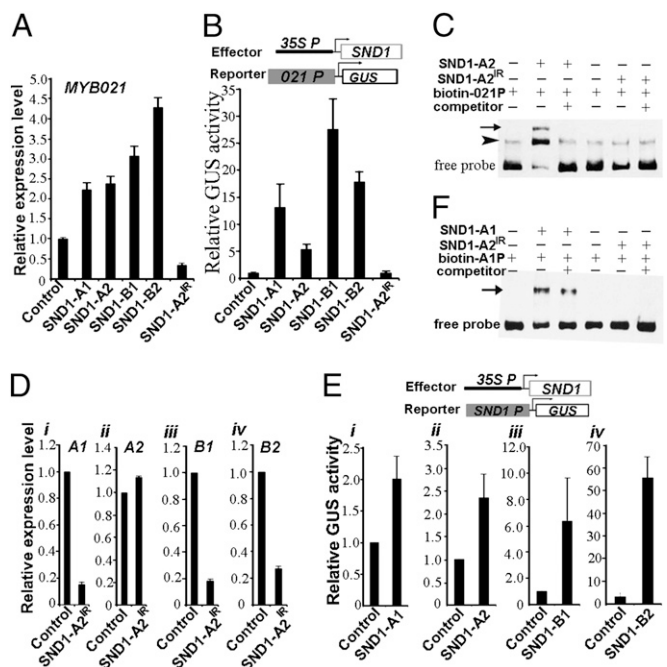


Fig. 2. PtrSND1-A2^{IR} inhibits expression of the *PtrMYB021* (*MYB021*) gene and the *PtrSND1* gene members. (A) qRT-PCR analysis of endogenous *MYB021* transcript abundance in *P. trichocarpa* SDX protoplasts overexpressing individually the five *PtrSND1* members. *pUC19-35S-sGFP* (25) was the control. (B) Effector–reporter-based gene transactivation assays in *Arabidopsis* leaf protoplasts. Only PtrSND1-A2^{IR} could not activate *PtrMYB021* promoter. Reporter construct alone was the control. (C) EMSA. The arrow shows the shifted complex, and the arrowhead indicates nonspecific binding. (D) Endogenous transcript abundance of the four *PtrSND1*s [A1 (i), A2 (ii), B1 (iii), and B2 (iv)] in *P. trichocarpa* SDX protoplasts overexpressing *PtrSND1-A2^{IR}*. *pUC19-35S-sGFP* was used as the control. (E) Effector–reporter-based gene transactivation assays show self-activation of four full-size *PtrSND1* members: A1 (i), A2 (ii), B1 (iii), and B2 (iv). Each reporter construct contains an ~2-kb promoter and cotransfected with the corresponding effector. Reporter construct alone was the control. (F) EMSA. The arrow shows the shifted complex. All control values in A, B, D, and E were set as 1. The error bars in A, B, D, and E represent SE of three biological replicates.

trichocarpa SDX protoplasts resulted in drastically reduced transcript abundances of the endogenous *PtrSND1-A1*, *-B1*, and *-B2*, but had essentially no effect on the expression of its full-size isoform, *PtrSND1-A2* (Fig. 2D). Because the transcript level of a gene is a function of the abundance of the TF that regulates the expression of the gene, the reduced expression of *PtrSND1-A1*, *-B1*, and *-B2* by PtrSND1-A2^{IR} suggests that PtrSND1-A2^{IR} inhibits the expression of the TF that regulates these genes. To test this suggestion, we first verified whether each of the four full-size PtrSND1 members is a TF activating its own gene. Many TFs in animals and plants regulate their own expression (self-activation or -repression) in addition to responding to other input signals (13, 27).

Transactivation assays confirmed that each of the four full-size PtrSND1 members could activate its own promoter (self-activation), indicated by induced β -glucuronidase (GUS) activity (Fig. 2E). Using EMSA, we further demonstrated that such self-activation is a result of direct binding of PtrSND1 to its own promoter (Fig. 2F and Fig. S4). These results strongly suggest that PtrSND1-A2^{IR} can suppress *PtrSND1-A1*, *-B1*, and *-B2* gene expression (Fig. 2D) through inhibiting the self-activation (Fig. 2E) of these *PtrSND1*s. The inability of PtrSND1-A2^{IR} to suppress *PtrSND1-A2* expression (Fig. 2D, ii) suggests that *PtrSND1-A2* is transactivated not only by its own protein (Fig. 2E, ii) but also by other unknown TFs or input signals. PtrSND1-A2^{IR} may attenuate the self-activation of *PtrSND1-A2* but have no effect

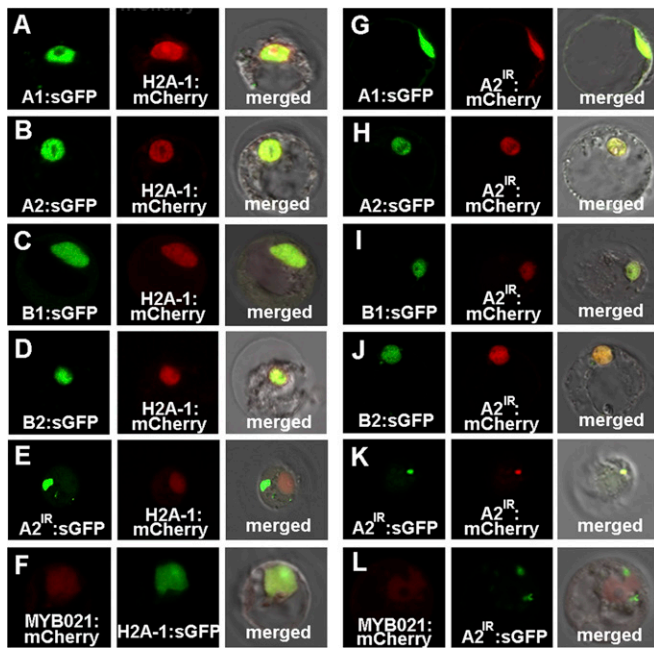


Fig. 3. Protein colocalization in *P. trichocarpa* SDX protoplasts demonstrate that PtrSND1-A2^{IR} is translocated from cytoplasmic foci to the nucleus by full-size PtrSND1 members. (A–F) Subcellular localization of five PtrSND1 fusion proteins: A1 (A), A2 (B), B1 (C), B2 (D), and A2^{IR} (E), and PtrMYB021 fusion protein, MYB021 (F). Each PtrSND1 was fused with sGFP and cotransferred with the nuclear marker H2A-1:mCherry (29) into SDX protoplasts. MYB021:mCherry and the nuclear marker H2A-1:sGFP were cotransferred. (G–J and L) Translocation of A2^{IR} from the cytoplasmic foci (E) into the nucleus (G–J) by the full-size PtrSND1 (G–J) but not MYB021 (L). (K) Without the full-size PtrSND1 carrier, A2^{IR} remains in the cytoplasm.

on *PtrSND1-A2* expression induced by other factors, resulting in an unchanged *PtrSND1-A2* transcript level (Fig. 2*D, ii*).

To further investigate the PtrSND1-A2^{IR}-mediated suppression of *PtrSND1* genes, we performed transactivation assays of PtrSND1-A2^{IR} on *PtrSND1* promoters. The results demonstrated that PtrSND1-A2^{IR} could not activate the promoters of *PtrSND1* member genes (Fig. S5), just as PtrSND1-A2^{IR} could not activate *PtrMYB021* (Fig. 2*B*). EMSA showed that the lack of such activation is because PtrSND1-A2^{IR} cannot bind to the promoters of *PtrSND1* or *PtrMYB021* (Fig. 2*C* and *F* and Fig. S4). These results suggest that the PtrSND1-A2^{IR}-mediated attenuation of *PtrSND1* and *PtrMYB021* gene expression (Fig. 2*A* and *D*) follows a similar mechanism where a direct binding of PtrSND1-A2^{IR} to the promoter of its target gene is not essential. By having a dimerization domain intact near the N terminus (Fig. 1*E, v*) (22, 26), PtrSND1-A2^{IR} may use its dimerization ability to prevent full-size PtrSND1 proteins from accomplishing their normal activation functions, leading to attenuated expression of *PtrSND1* and *PtrMYB021* (Fig. 2*A* and *D*).

PtrSND1-A2^{IR} acts as a unique gene repression mediator, regulating the *SND1* transcriptional network in *P. trichocarpa*. PtrSND1-A2^{IR} is neither an active nor a passive repressor, such as VNI2, which reduces VND7 transactivation activity as a regulator of *VND7* (28). However, our results strongly suggest the involvement of specific protein–protein interactions in the PtrSND1-A2^{IR} transcriptional regulation. We then investigated the subcellular localization of all five PtrSND1 members, as well as specific dimerization and subcellular locations of these dimers.

PtrSND1-A2^{IR} Is in Cytoplasmic Foci and the Four Full-Size PtrSND1s Are in the Nucleus of *P. trichocarpa* SDX Cells. We used fluorescent proteins to reveal the subcellular location of PtrSND1 members in *P. trichocarpa* SDX protoplasts. We cotransfected the protoplasts

with *35S-PtrSND1:sGFP* and *35S-H2A-1:mCherry* nuclear marker plasmids (29) and demonstrated that each of the four full-size PtrSND1s colocalizes with the marker in the nucleus (Fig. 3*A–D*). Exclusive nuclear location of these four PtrSND1s was observed for 85–95% of the transfected protoplasts examined, whereas in the remaining protoplasts, PtrSND1s were found in both nucleus and cytoplasmic foci. PtrMYB021 was also predominantly in the nucleus (Fig. 3*F*).

In sharp contrast to the nuclear location of the full-size PtrSND1s, cotransfection of *35S-PtrSND1-A2^{IR}:sGFP* and *35S-H2A-1:mCherry* plasmids demonstrated that the splice variant PtrSND1-A2^{IR} was located exclusively in small punctate structures in the cytoplasm of the protoplasts (Fig. 3*E*). The exclusive location of PtrSND1-A2^{IR} in cytoplasmic foci and sporadically abnormal residence of PtrSND1s in these foci suggest that PtrSND1-A2^{IR} may retain these PtrSND1s in the cytoplasm through protein–protein interactions. If PtrSND1-A2^{IR} interacts with any PtrSND1, these proteins should be colocalized. We then performed protein subcellular colocalization experiments.

Cytoplasmic PtrSND1-A2^{IR} Can Be Translocated into the Nucleus by Full-Size PtrSND1s. To colocalize PtrSND1-A2^{IR} with each of the five PtrSND1 members, we prepared a *35S-PtrSND1-A2^{IR}:mCherry* fusion gene construct and cotransferred it with each of the *35S-PtrSND1:sGFP* constructs into *P. trichocarpa* SDX protoplasts. Unexpectedly, in the presence of any one of the four full-size PtrSND1 members, PtrSND1-A2^{IR} was translocated from the cytoplasmic foci (Fig. 3*E*) to the nucleus, demonstrated by the nuclear colocalization of PtrSND1-A2^{IR} (mCherry) with each of the four full-size PtrSND1s (sGFP) (Fig. 3*G–J*). Such translocation of PtrSND1-A2^{IR} was exclusive to all cotransfected protoplasts.

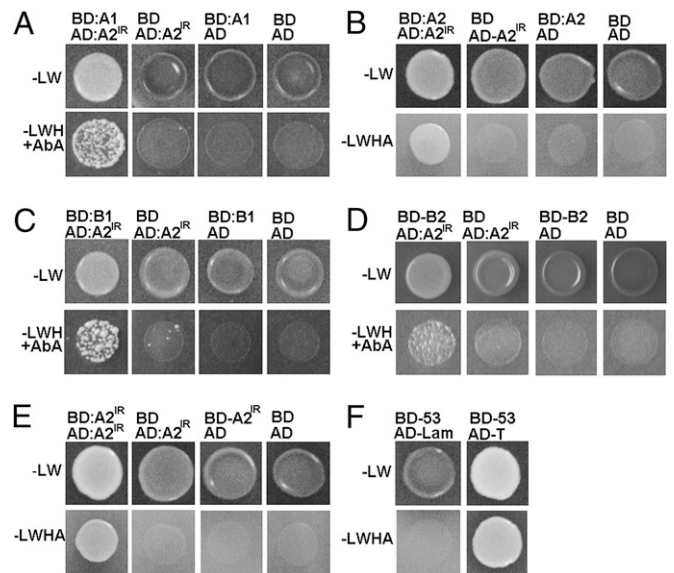


Fig. 4. Y2H demonstrates that PtrSND1-A2^{IR} interacts with each of the five PtrSND1s. The full-size A2^{IR} and the NAC-domain from A1, A2, B1, and B2 were each fused to the Gal4 binding domain (BD) to make BD:A2^{IR}, and BD:A1, BD:A2, BD:B1, and BD:B2 fusions as the bait. Each bait and prey (AD:A2^{IR}) pair was cotransfected into yeast cells and selected on the SD/–Leu/–Trp (–LW) medium. (B and E) A2^{IR}/A2^{IR} or A2^{IR}/A2 protein–protein interaction was validated by the growth of the transformants on the SD/–Leu/–Trp/–His/–Ade (–LWHA) medium. (A, C, and D) Positive A1/A2^{IR}, B1/A2^{IR}, and B2/A2^{IR} interactions were validated by using the SD/–Leu/–Trp/–His/–Aba (–LWH+AbA) selection medium. (F) The positive growth was confirmed by the positive control BD-53/AD-T. BD/AD:A2^{IR}, BD:SND1/AD, or BD/AD did not grow on the selection medium (A–E), as indicated by the negative control, BD-53/AD-Lam (F).

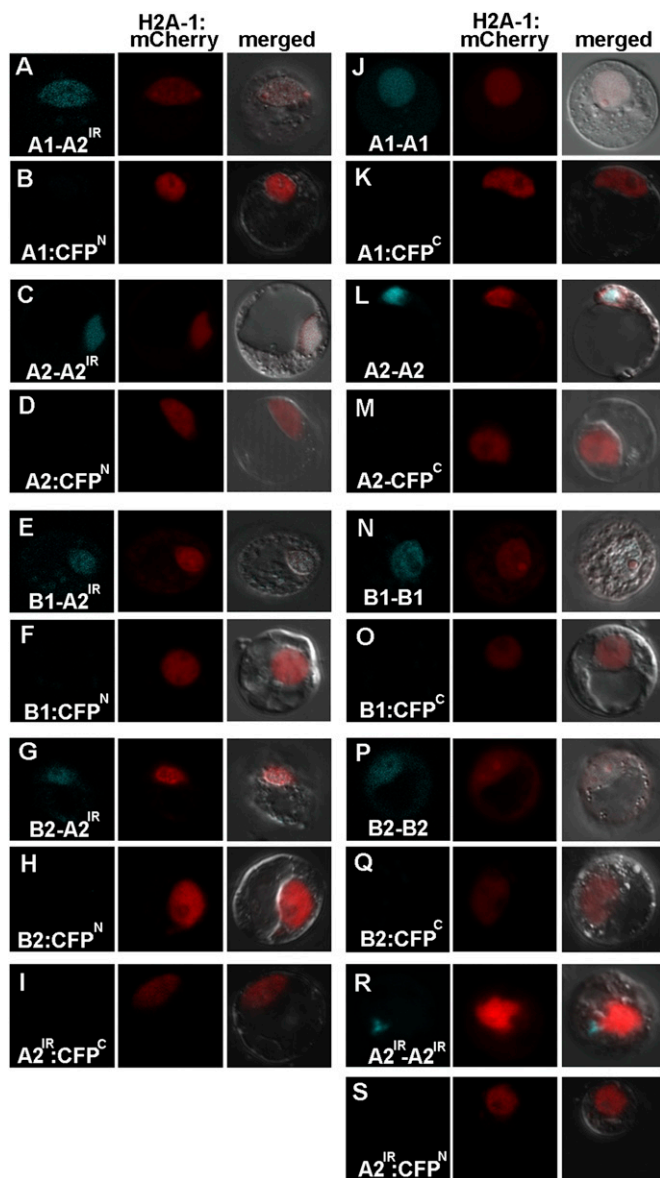


Fig. 5. BiFC in *P. trichocarpa* SDX protoplasts demonstrates that A2^{IR} heterodimerizes with the four full-size PtrSND1s and that all five PtrSND1s homodimerize. (A, C, E, and G) A2^{IR}:CFP^N cotransformed with A1:CFP^N (A), A2:CFP^N (C), B1:CFP^N (E), or B2:CFP^N (G) into SDX protoplasts give positive BiFC signals that were colocalized with the marker H2A-1 (29) in the nucleus. (J, L, N, and P) Similarly, positive BiFC signals for homodimers of the four full-size PtrSND1s were colocalized with H2A-1 in the nucleus. (R) Cotransformation of A2^{IR}:CFP^C and A2^{IR}:CFP^N gave BiFC signals exclusively in the cytoplasmic foci. (B, D, F, H, I, K, M, O, Q, and S) As negative controls, transformation of A2^{IR}:CFP^C (I), A2^{IR}:CFP^N (S), A1:CFP^N (B), A1:CFP^C (K), A2:CFP^N (D), A2:CFP^C (M), B1:CFP^N (F), B1:CFP^C (O), B2:CFP^N (H), or B2:CFP^C (Q) alone did not give any CFP signals. In all BiFC experiments, the nuclear marker H2A-1:mCherry was cotransferred.

Cotransfection of SDX protoplasts with 35S-PtrSND1-A2^{IR}:mCherry and 35S-PtrSND1-A2^{IR}:sGFP showed that sGFP and mCherry signals, both representing PtrSND1-A2^{IR}, remained entirely colocalized in cytoplasmic foci (Fig. 3K). As a control experiment, we cotransfected the protoplasts with 35S-PtrSND1-A2^{IR}:sGFP and 35S-PtrMYB021:mCherry and demonstrated that PtrSND1-A2^{IR} remained exclusively in cytoplasmic foci, whereas PtrMYB021 was in the nucleus (Fig. 3L). Therefore, PtrSND1-A2^{IR} can only be translocated into the nucleus by a full-size PtrSND1 carrier, not just any TF proteins.

Y2H Demonstrates That PtrSND1-A2^{IR} Dimerizes with Five PtrSND1 Members. We next performed Y2H assays to test whether PtrSND1-A2^{IR} can dimerize with the carrier PtrSND1 for translocation into the nucleus. Each of the four full-size PtrSND1s heterodimerized with PtrSND1-A2^{IR} (Fig. 4A–D), and PtrSND1-A2^{IR} self-interacted (Fig. 4E). The interactions for the PtrSND1-A2^{IR}/PtrSND1-A2 (A2^{IR}/A2; Fig. 4B) and the A2^{IR}/A2^{IR} (Fig. 4E) dimers were stronger than those for the A2^{IR}/A1, A2^{IR}/B1, and A2^{IR}/B2 heterodimers. The heterodimerization in yeast and the nuclear colocalization in protoplasts (Fig. 3G–J) of two proteins [(A2^{IR} and A1), (A2^{IR} and A2), (A2^{IR} and B1), and (A2^{IR} and B2)] are strong evidence that the pairs of proteins exist as heterodimers in plant nuclei. To further test this inference, we performed BiFC assays in *P. trichocarpa* SDX protoplasts.

BiFC Identifies PtrSND1/PtrSND1-A2^{IR} Heterodimers in the Nucleus of SDX Cells. Using BiFC, we tested for heterodimers between PtrSND1-A2^{IR} and each of the four full-size PtrSND1s, and all possible homodimers from the five PtrSND1s. Different combinations of two plasmids, each containing a target protein fused at the N terminus to one of two complementing segments of CFP—CFP^N (aa 1–173) and CFP^C (aa 174–329)—were cotransformed together with the H2A-1:mCherry nuclear marker plasmid into SDX protoplasts. A2^{IR} heterodimerized with each of the full-size PtrSND1s, and these heterodimers (A2^{IR}/A1, A2^{IR}/A2, A2^{IR}/B1, and A2^{IR}/B2) colocalized with the H2A-1:mCherry marker nearly exclusively in the nucleus (Fig. 5A–I). The four full-size PtrSND1s homodimerized, and these dimers (A1/A1, A2/A2, B1/B1, and B2/B2) were also nucleus specific (Fig. 5J–Q). A2^{IR}/A2^{IR} homodimers were exclusively in cytoplasmic foci (Fig. 5R, S, and I), validating the PtrSND1-A2^{IR} colocalization results (Fig. 3K) and the finding that the translocation of PtrSND1-A2^{IR} into the nucleus requires a full-size PtrSND1.

The results with RNA-Seq, protein gel blotting, transgene transcriptional regulation, gene transactivation, EMSA, protein subcellular localization and colocalization, Y2H, and BiFC provide strong evidence for unique NAC transcriptional regulation, in which a cytoplasmic splice variant, PtrSND1-A2^{IR}, is translocated by its full-size family members into the nucleus for repressing the expression of these members and their direct target genes.

Discussion

Complex biological processes in growth and development, such as secondary cell wall or wood formation, are regulated at many levels (a hierarchy) by transacting elements (30). SND1s are an essential part of such a hierarchical network. Although SND1s' downstream targets have been studied extensively, their upstream regulators (for activation or repression) have not previously been identified (6). Repression is as necessary as activation in transcriptional control for growth and development, and it is frequently achieved through dominant-negative TFs (10, 14, 17). In plants, alternative splicing-generated dominant-negative TFs that can act as an individual antagonist against multiple target gene products have not been reported. A dominant-negative TF that can antagonize its own family members on their self-activation is also previously unknown in plants.

In this study, we showed that a naturally occurring, SDX-specific splice variant, PtrSND1-A2^{IR}, is a dominant-negative regulator. It antagonizes the autoregulation of its family members (Fig. 2D) as well as the activation of their common target *PtrMYB021* (Fig. 2A). We reported here several distinct mechanisms of PtrSND1 regulation. Typically, a dominant-negative TF lacks a DNA-binding domain (10, 16, 17). PtrSND1-A2^{IR} has the β1 and β2 subdomains (Fig. 1E, v) believed necessary for DNA binding, but lacks the β6 subdomain. However, EMSA demonstrated that PtrSND1-A2^{IR} does not bind to promoters of *PtrSND1* member and *PtrMYB021* genes (Fig. 2C and F and Fig. S4). The inclusion of the β6 region, in addition to β1 and β2, in the β-sheet structure may be important for DNA binding. Although PtrSND1-A2^{IR} lacks DNA-binding ability, it dimerizes (Fig. 5) because it retains the N-terminal dimerization domain (Fig. 1E, v).

Although homodimers of full-size PtrSND1 members are nucleus specific (Fig. 5 *J–Q*), PtrSND1-A2^{IR} remained exclusively in the cytoplasm as homodimers or monomers (Figs. 3*E* and 5*R*). The cytoplasmic foci location of PtrSND1-A2^{IR} suggests that this protein is involved in posttranscriptional degradation of its target RNAs (31). However, there is no RNA-binding motif in PtrSND1-A2^{IR} that would indicate a degradation mechanism. Instead, PtrSND1-A2^{IR} is translocated into the nucleus as a heterodimeric partner with any of its full-size PtrSND1 family members (Figs. 3 *G–J* and 5 *A–I*). The formation of these heterodimers must occur in the cytoplasm because PtrSND1-A2^{IR} monomers or homodimers are not available in the nucleus. This subcellular translocation of a splice variant is unique and may represent an integral part of the nucleocytoplasmic transport required for the SND1 transcriptional regulation.

In the nucleus, the PtrSND1-A2^{IR}/PtrSND1 heterodimer has only one functional DNA-binding structure (from the full-size PtrSND1), instead of the required two. Consequently, the defective DNA-binding system may disrupt subsequent gene transactivation, resulting in suppressed self-activation of *PtrSND1s* (Fig. 2*D*). The suppressed level of *PtrSND1s* would then lead to reduced transactivation of their target genes, such as *PtrMYB021*, resulting in attenuated transcript levels of *PtrMYB021*, as observed in SDX protoplasts in which *PtrSND1-A2^{IR}* is overexpressed (Fig. 2*A*). It is also possible that the defective DNA-binding system created by the PtrSND1-A2^{IR}/PtrSND1 heterodimer directly disrupted the normal PtrSND1-mediated transactivation of *PtrMYB021*, causing a reduced level of *PtrMYB021* transcripts (Fig. 2*A*).

In addition to the dual DNA-binding specificity, a set of two transactivation or transrepression domains through dimerization is also necessary for TFs to be fully functional in regulating target gene expression (10, 14, 16, 17). The PtrSND1-A2^{IR}/PtrSND1 heterodimer has only one transactivation domain, further disrupting the normal PtrSND1 functions to result in inhibited expression of *PtrSND1* and *PtrMYB021* genes (Fig. 2*A* and *D*). This

mechanism may also explain the repressed vessel differentiation due to inhibited *VND7* function in *Arabidopsis* in which an artificially truncated *VND7* lacking the transactivation domain was overexpressed (9). These inhibition mechanisms have been well characterized for many dominant-negative repressors. Among the best-studied repressors are the members of the Id (inhibitor of DNA-binding) subfamily of basic helix–loop–helix TFs involved in cell cycle and tumorigenesis in animals (18). Ids lack a DNA-binding region, and, consequently, they disrupt the function of other bHLH TFs, making them nonproductive through dimerization (18).

The formation of nonproductive PtrSND1-A2^{IR}/PtrSND1 heterodimers would also prevent full-size PtrSND1s from dimerizing to generate functional complexes. This sequestration of functional PtrSND1s together with the dominant-negative effects of PtrSND1-A2^{IR} may efficiently maintain transcriptional homeostasis in the SND- and VND-regulated networks. A few such dominant negatives may have evolved from genome duplication in woody plants to dampen adverse effects due to transcriptional redundancy. PtrSND1-A2^{IR} has provided an entry to discovering more about the upstream regulation of SND and VND and to reveal the comprehensive hierarchical network regulating wood formation.

Materials and Methods

Plant materials, PCR cloning, RNA-Seq, and 3'RACE, qRT-PCR, SDS/PAGE, Western blotting, *P. trichocarpa* SDX protoplast preparation/transfection, gene transactivation assays, plasmid constructions, EMSA, Y2H, and BiFC are described in detail in *SI Materials and Methods*. They are described in the sequence shown above. All primer sequences are listed in Table S1.

ACKNOWLEDGMENTS. We thank Kyung-Hwan Han and Won-Chan Kim for analyzing the PtrSND1-A2^{IR} for RNA binding motifs. This work was supported by the Office of Science (Biological and Environmental Research), Department of Energy Grant DE-SC000691 (to V.L.C.). X.-H.Z. thanks the sabbatical support of the North Carolina State University Jordan Family Endowment.

- Evert RF (2006) *Esau's Plant Anatomy: Meristems, Cells, and Tissues of the Plant Body: Their Structure, Function, and Development* (Wiley & Sons, Hoboken, NJ), 3rd Ed.
- Ohtani M, et al. (2011) A NAC domain protein family contributing to the regulation of wood formation in poplar. *Plant J* 67:499–512.
- Zhong R, McCarthy RL, Lee C, Ye ZH (2011) Dissection of the transcriptional program regulating secondary wall biosynthesis during wood formation in poplar. *Plant Physiol* 157:1452–1468.
- Ko JH, Yang SH, Park AH, Lerouxel O, Han KH (2007) ANAC012, a member of the plant-specific NAC transcription factor family, negatively regulates xylary fiber development in *Arabidopsis thaliana*. *Plant J* 50:1035–1048.
- Demura T, Ye ZH (2010) Regulation of plant biomass production. *Curr Opin Plant Biol* 13:299–304.
- Wang HZ, Dixon RA (2012) On-off switches for secondary cell wall biosynthesis. *Mol Plant* 5:297–303.
- Zhong R, Demura T, Ye ZH (2006) SND1, a NAC domain transcription factor, is a key regulator of secondary wall synthesis in fibers of *Arabidopsis*. *Plant Cell* 18:3158–3170.
- Kubo M, et al. (2005) Transcription switches for protoxylem and metaxylem vessel formation. *Genes Dev* 19:1855–1860.
- Yamaguchi M, Kubo M, Fukuda H, Demura T (2008) Vascular-related NAC-DOMAIN7 is involved in the differentiation of all types of xylem vessels in *Arabidopsis* roots and shoots. *Plant J* 55:652–664.
- Klemm JD, Schreiber SL, Crabtree GR (1998) Dimerization as a regulatory mechanism in signal transduction. *Annu Rev Immunol* 16:569–592.
- Nigg EA (1997) Nucleocytoplasmic transport: Signals, mechanisms and regulation. *Nature* 386:779–787.
- Xie Q, Frugis G, Colgan D, Chua NH (2000) *Arabidopsis* NAC1 transduces auxin signal downstream of TIR1 to promote lateral root development. *Genes Dev* 14:3024–3036.
- Wang H, Zhao Q, Chen F, Wang M, Dixon RA (2011) NAC domain function and transcriptional control of a secondary cell wall master switch. *Plant J* 68:1104–1114.
- Gaston K, Jayaraman P-S (2003) Transcriptional repression in eukaryotes: Repressors and repression mechanisms. *Cell Mol Life Sci* 60:721–741.
- Seo PJ, Hong SY, Kim SG, Park CM (2011) Competitive inhibition of transcription factors by small interfering peptides. *Trends Plant Sci* 16:541–549.
- Müller CW (2001) Transcription factors: Global and detailed views. *Curr Opin Struct Biol* 11:26–32.
- Amoutzias GD, Robertson DL, Van de Peer Y, Oliver SG (2008) Choose your partners: Dimerization in eukaryotic transcription factors. *Trends Biochem Sci* 33:220–229.
- Ruzinova MB, Benezra R (2003) Id proteins in development, cell cycle and cancer. *Trends Cell Biol* 13:410–418.
- Seo PJ, Kim MJ, Ryu JY, Jeong EY, Park CM (2011) Two splice variants of the IDD14 transcription factor competitively form nonfunctional heterodimers which may regulate starch metabolism. *Nat Commun* 2:303.
- Seo PJ, et al. (2012) A self-regulatory circuit of CIRCADIAN CLOCK-ASSOCIATED1 underlies the circadian clock regulation of temperature responses in *Arabidopsis*. *Plant Cell* 24:2427–2442.
- Zhong R, Lee C, Ye ZH (2010) Functional characterization of poplar wood-associated NAC domain transcription factors. *Plant Physiol* 152:1044–1055.
- Ernst HA, Olsen AN, Larsen S, Lo Leggio L, Lo Leggio L (2004) Structure of the conserved domain of ANAC, a member of the NAC family of transcription factors. *EMBO Rep* 5:297–303.
- Zhong R, Richardson EA, Ye ZH (2007) The MYB46 transcription factor is a direct target of SND1 and regulates secondary wall biosynthesis in *Arabidopsis*. *Plant Cell* 19:2776–2792.
- Ko JH, Kim WC, Han KH (2009) Ectopic expression of MYB46 identifies transcriptional regulatory genes involved in secondary wall biosynthesis in *Arabidopsis*. *Plant J* 60:649–665.
- Chen HC, et al. (2011) Membrane protein complexes catalyze both 4- and 3-hydroxylation of cinnamic acid derivatives in monolignol biosynthesis. *Proc Natl Acad Sci USA* 108:21253–21258.
- Puranik S, Sahu PP, Srivastava PS, Prasad M (2012) NAC proteins: Regulation and role in stress tolerance. *Trends Plant Sci* 17:369–381.
- Becskei A, Serrano L (2000) Engineering stability in gene networks by autoregulation. *Nature* 405:590–593.
- Yamaguchi M, et al. (2010) VND-INTERACTING2, a NAC domain transcription factor, negatively regulates xylem vessel formation in *Arabidopsis*. *Plant Cell* 22:1249–1263.
- Tenea GN, et al. (2009) Overexpression of several *Arabidopsis* histone genes increases agrobacterium-mediated transformation and transgene expression in plants. *Plant Cell* 21:3350–3367.
- Yu H, Gerstein M (2006) Genomic analysis of the hierarchical structure of regulatory networks. *Proc Natl Acad Sci USA* 103:14724–14731.
- Macara IG (2001) Transport into and out of the nucleus. *Microbiol Mol Biol Rev* 65:570–594.